

## **AN ASSESSMENT OF THE HIGH-TEMPERATURE OXIDATION BEHAVIOR OF Fe-Cr STEELS IN WATER VAPOR AND STEAM**

I. G. Wright and B. A. Pint  
Oak Ridge National Laboratory  
Oak Ridge, Tennessee

### **ABSTRACT**

European and Japanese developments of technologies for coal-fired power plants employing advanced steam conditions have resulted in Fe-Cr alloys that appear to have acceptable strength up to 620°C (1148°F) or possibly 650°C (1202°F). However, these alloys have relatively low Cr contents (up to 13 percent), which are marginal for the formation of protective oxide scales at these temperatures. Since there is no practical experience with alloys of this type in steam at elevated temperatures, information on their oxidation behavior in steam, in particular their rate of oxidation, is needed. This paper reports an assessment of the available information on steam oxidation of Fe-Cr alloys. It appears that the 9-12Cr and the 2-3Cr alloys oxidize at essentially the same rate at 550°C (1022°F), but the higher-Cr alloys provide somewhat better protection at the higher temperatures of interest (up to 700°C/1292°F). However, the oxidation rates are still fast, since the predominant scales formed are based on magnetite. It will be important for lifetime prediction to determine if the scale grows according to a parabolic or linear rate law; this point is not well resolved by examination of existing data. Routes for promoting the formation of more protective, Cr-rich scales on the more highly-alloyed are being explored and some show good promise.

Keywords: ferritic steels; steam oxidation; magnetite scales; parabolic oxidation; linear oxidation; advanced steam conditions

### **INTRODUCTION**

In recent years, interest in the development of steam-generating power plants with increased efficiencies has led to the consideration of materials capable of operating at steam temperatures and pressures significantly higher than those employed in current power plants. Since the efficiency of a

Rankine cycle system increases with increasing temperature difference between the high-temperature source (steam) and the heat sink (condenser), the most obvious route to increasing the efficiency of steam power plants is to increase the maximum steam temperature capability. The net efficiency of modern coal-fired, steam-generating power plants in the U.S. typically is approximately 40 percent. While efficiencies of greater than 50 percent are claimed by a few steam generators, much of the efficiency increase is due to the availability of very cold cooling water at their specific locations (for example, the Baltic Sea). On-going programs in Europe<sup>(1)</sup> and Japan<sup>(2)</sup> envision steam conditions increasing in stages to attain plant efficiencies of the order of 50 percent without special siting. The overall approach to materials application is to make use of ferritic steels to the maximum possible temperature before switching to higher-temperature alloys. If possible, it would be preferable to avoid austenitic steels because of their lower thermal conductivity, higher coefficient of thermal expansion and higher density, as well as difficulties with dissimilar metal welds. The alternative to austenitic steels is to use Ni-based alloys although the associated increased cost must be justified. The high-temperature Ni-based alloys also have lower thermal conductivity than the ferritic steels, but are less susceptible to thermal fatigue than the austenitic steels.

Because of the issues discussed above, there is emphasis in current research programs on improving the high-temperature creep properties of ferritic steels containing 10-12 percent (by weight) Cr. The goal of the European COST-522 program on advanced steam power plants is the identification of materials for use in steam at 650°C/296 atm (1202°F/4,350 psi) while the Japanese national program has a goal of 650°C/349 atm (1202°F/5,135 psi), and the European Thermie program is aimed at 700°C/388 atm (1292°F/5,440 psi) steam. Higher-temperature and pressure steam conditions also are under consideration in the U.S. as part of the Department of Energy's Vision 21 program, which is intended to foster the development of clean and efficient coal-fired power plants; some cycle analyses have featured steam temperatures of 760 and 871°C (1400 and 1600°F).

Current Fe-Cr alloys containing 2-3 percent Cr are limited in boiler service to temperatures of 580-600°C (1076-1112°F) on account of oxidation loss from the fireside environment, under conditions where wustite is unlikely to form. The temperature limits imposed by the U.S. boiler makers on the 300-series stainless steels (17-19 percent Cr) range from 700°C (1292°F) up to the ASME Boiler and Pressure Vessel Code creep rupture-based limit of 816°C (1500°F).

Developmental ferritic alloys in the 10-13Cr class appear to be capable of use up to approximately 620°C (1148°F)<sup>(1)</sup> at the stress levels of interest. However, the relatively low Cr content of these alloys raises concerns about their environmental resistance at the higher temperatures. Efforts have been initiated to generate information on the fireside and steam-side corrosion behavior of these materials, with most emphasis on fireside conditions. However, there is particular interest in the steam-side corrosion behavior, since early systematic studies<sup>(3,4)</sup> of model Fe-Cr alloys suggested that linear kinetics prevailed at temperatures above 700°C for Cr levels in the range 1-15 percent. Recent studies have tended to suggest that parabolic kinetics prevail at temperatures up to 700°C. Further, it appears that the protective behavior associated with the formation of a continuous Cr<sub>2</sub>O<sub>3</sub> layer is not necessarily observed in steam at alloy Cr levels below approximately 20 percent. The questions concerning the oxidation rate law to be applied as a function of temperature and alloy Cr level, and the Cr level needed for protective behavior in steam, must be resolved to allow reliable prediction of the service lifetimes of this class of alloys and the confidence in the application.

## BACKGROUND

Components for steam generators are designed for a finite service lifetime (normally 250,000 h), and materials selection is based primarily on creep properties and on the ability to resist metal section loss in the environment. Since alloy property measurements, at least prior to the finalization of the materials selection, involve relatively short-term testing coupled with extrapolation to the design lifetime, an accurate knowledge of the temperature-dependence of the oxidation behavior of alloys in steam is of considerable importance. While most of the oxidation studies in steam at temperatures below 700°C have reported that the oxidation behavior follows a parabolic rate law, two studies using model alloys in water vapor-Ar mixtures<sup>(3-5)</sup> have reported linear kinetics for Fe-Cr alloys containing up to 15 percent Cr over temperatures in the range 700 to 1200°C (1292 to 2192°F). These data were supported by morphological studies that confirmed that the oxidation behavior did not correspond to a parabolic rate law. In addition, Potter and Mann<sup>(6)</sup> reported that, under certain aqueous conditions at 300-400°C (572-752°F), magnetite growth on mild steel occurred at a linear rate, with the bulk of the scale growth occurring at the metal-oxide interface; the resulting scale was non-protective.

The experience from steam generator operation is that, for lower-Cr ferritic alloys (typically 0-2.25Cr), the oxidation rate at metal temperatures below approximately 580°C (1076°F) is parabolic initially but, as a result of the formation of multilayered scales, the growth rate changes to linear. There are fewer data for the oxidation of Fe-9Cr, which has been used extensively in recent years in superheater applications. Since Fe-10Cr-based alloys are expected to retain the ferritic structure up to approximately 850°C (1562°F), and the Fe-12Cr alloys up to 900°C (1652°F), the associated rapid Cr diffusion in the alloy provides the possibility that they will form relatively slower-growing, Cr-rich scales. Power plant experience with the higher-Cr austenitic alloys (types 304, 316, 321 and 347 steels) is that they exhibit slower oxidation rates than the low-Cr ferritics used to date, due to the formation of more protective (Cr-containing) scales. When scale exfoliation occurs from these alloys, the extent typically is less and only the outer magnetite layer is lost. As a result, the overall oxidation rate of these alloys in steam often is closer to parabolic than linear. However, Griess et al.<sup>(15,16)</sup> did not observe any scale spallation from type 304 in plant tests for longer than 20 kh, even though a transition from parabolic to linear kinetics occurred at approximately 8 kh, and porosity was noted in the magnetite layer after approximately 28 kh.

The bulk of the practical experience of the interaction of ferritic steels with steam is at temperatures less than 566°C (1050°F) and pressures of less than 177 atm (2,600 psi) or, for units operating at supercritical steam conditions, 238 atm (3,500 psi). In addition, two power plants operated in the U.S. for some time at higher steam temperatures and pressures: the Philo plant of American Electric Power [620°C/314 atm (1148°F/4,617 psi)] and the Eddystone plant of Philadelphia Electric [649°C/340 atm (1200°F/5,000 psi)]. Continuing interest in Europe and Japan has led to the introduction of plants operating at steam conditions of 566°C and 257 atm (1050°F, 3,770 psi), while the goal of ongoing development programs is steam conditions of up to 700°C (1292°F) and 350 atm (5,165 psi).

## THERMODYNAMIC CONSIDERATIONS

When considering the likely corrosion behavior of alloys in steam, it is first useful to examine the types of oxide scales likely to form in the environment as a function of metal temperature and steam pressure. It is well known<sup>(17)</sup> that in air, carbon steel forms two oxides: Fe<sub>3</sub>O<sub>4</sub> (magnetite) as an inner layer with Fe<sub>2</sub>O<sub>3</sub> (haematite) at the gas interface at temperatures up to approximately 550°C (1022°F). With increasing alloy Cr content, a Cr-rich spinel phase of variable stoichiometry, FeFe<sub>2-x</sub>Cr<sub>x</sub>O<sub>4</sub>, forms at the metal-oxide interface; the diffusion of cations through this spinel is significantly reduced, and the

oxidation rate is slowed. At sufficiently high Cr levels (depending on temperature) Cr content of this layer increases and eventually the formation of  $\text{Cr}_2\text{O}_3$ , which grows at an appreciably slower rate, is possible. In air, the oxidation rate decreases sharply with increasing Cr content from 2 to 10 percent.

Figure 1 shows the equilibrium dissociation oxygen partial pressures of the oxides and steam, assuming that the dissociation via  $\text{H}_2\text{O} = \text{H}_2 + 1/2\text{O}_2$  goes to equilibrium at the metal-steam interface, as a function of temperature. An important point is that FeO (wustite) becomes stable in the temperature range of interest for advanced steam plants; this oxide is intrinsically more defective than  $\text{Fe}_3\text{O}_4$ , and so will support significantly faster oxidation rates. The stability of FeO also is dependent on the Cr content of the alloy, and there is a minimum level at which it will not be formed.

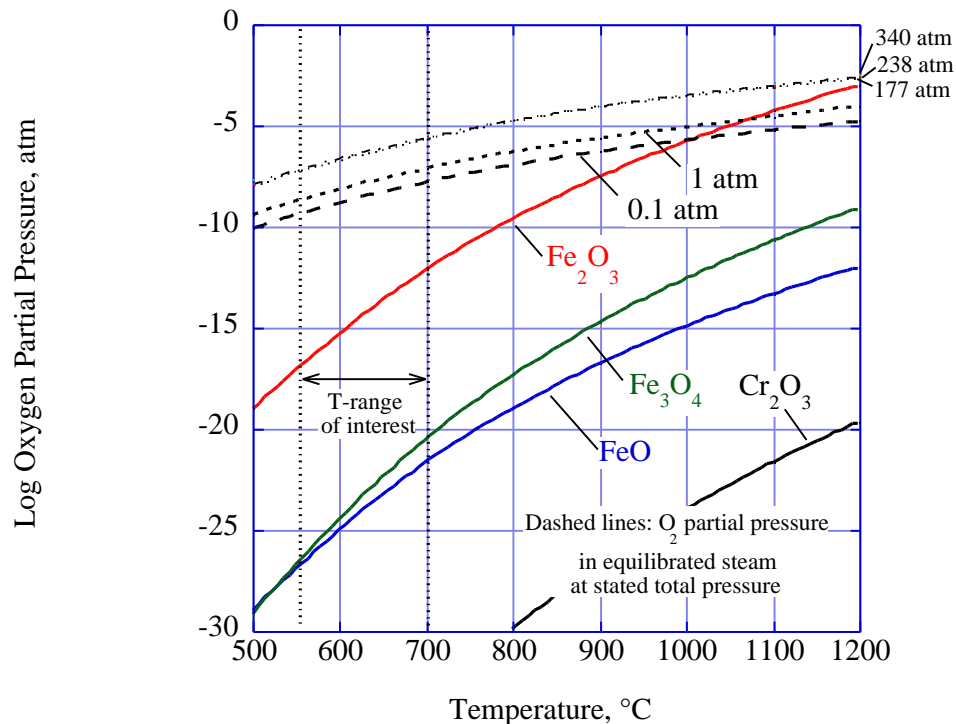


FIGURE 1. Effective Oxygen Partial Pressures in Steam, and the Stability of the Oxides of Interest

While decreasing the steam pressure from 340 atm to 0.1 atm results in a significant decrease in the equilibrium partial pressure of oxygen in the steam from, for example at 700°C,  $3.8 \times 10^{-6}$  atm to  $1.7 \times 10^{-8}$  atm, these oxygen partial pressures are still some four orders of magnitude higher than the dissociation oxygen partial pressure of the least stable iron oxide,  $\text{Fe}_2\text{O}_3$ , so that it would be expected that the same oxides would be present in scales grown at either pressure extreme if the steam were equilibrated on the metal-oxide surfaces. It is noteworthy that  $\text{Fe}_2\text{O}_3$  becomes unstable in 0.1 atm steam at temperatures above approximately 1000°C, and in 1 atm steam at temperatures above approximately 1075°C. While  $\text{Fe}_3\text{O}_4$  would be expected to be a stable phase under all conditions considered here, the laboratory studies<sup>(3-5)</sup> that used Ar-0.1 water vapor mixtures at the higher temperatures reported that the scales formed were essentially only FeO, suggesting that in those cases the oxidation processes were controlled by the kinetics of delivery of water vapor molecules to the oxide surface and their dissociation.

In power plant practice, oxygen-scavenging agents such as hydrazine are added to the boiler feed water to inhibit aqueous corrosion of the low-alloy steel used in the lower-temperature parts of the steam

circuit. A trend in supercritical steam generators has been to replace such oxygen scavenging with precise control of the oxygen content of the boiler feed water, typically at a level of 5 ppb by weight. The oxygen is intended to control the dissolution of iron in the feedwater and so minimize the deposition of a thermally-insulating porous layer of magnetite in the evaporator tubes. In that case, the effective oxygen partial pressure in the fluid leaving the evaporator tube bank would be expected to be set by the equilibrium dissociation partial pressure of magnetite at approximately 450°C, i.e.,  $9 \times 10^{-33}$  atm. However, this practice is unlikely to affect the oxidation potential of the steam produced, since such oxygen levels are significantly lower than the  $pO_2$  set by the equilibrium dissociation of steam (see Figure 1).

## ALLOYS

The alloys of interest are the newly-developed W-containing 2-3Cr alloys (such as ST22 and HCM2S), which are expected to form magnetite-dominated scales, and the advanced 10-12Cr steels such as HCM12A, which are expected to form (Fe,Cr) oxides rather than  $Cr_2O_3$  scales. The chemical compositions of these and other relevant alloys are shown in Table I.

TABLE I  
NOMINAL ALLOY COMPOSITIONS (IN WEIGHT PERCENT)

Alloy	Ni	Cr	Si	Mn	Mo	W	V	Nb	Cu	C	N
HCM2S		2.17	0.21	0.49	0.11	1.59	0.23	0.05		0.05	
ST22		2.2			0.1	1.5					
P91	0.04	9	0.35	0.45	0.95		0.22	0.08		0.1	0.03-0.07
E911	0.2	9		0.5	1	1	0.2	0.08		0.1	0.05
NF616 (P92)	0.04	8.5-9.5	0.5	0.3-0.6	0.3-0.6	1.5-2.0	0.15-0.25	0.04-0.09		0.07-0.13	0.03-0.07
HCM12A	0.5	10-12.5	0.5	0.7	0.25-0.6	1.5-2.5	0.15-0.3	0.04-0.1	0.3-1.7	0.12	0.04-0.1

## OXIDATION KINETICS

Table II summarizes the range of temperatures and pressures used in the pertinent studies of steam oxidation of alloys of potential interest for steam generator applications. While many of the studies addressed the effects of higher metal temperatures than currently employed, it is noteworthy that only two laboratory studies employed steam pressures that corresponded to supercritical conditions (greater than 374.1°C, 218 atma., for pure water), and these were completed at least 24 years ago so are not necessarily concerned with alloys of current interest.

### Effect of Steam Temperature

Measurements of oxide scale thicknesses in superheater and reheater tubes taken from U.S. steam generators indicate that, at metal temperatures below approximately 580°C (1076°F), the oxidation rate of alloys containing up to 2.25 percent Cr follows a parabolic rate law up to approximately 8 to 10 kh, but at longer times the overall growth rate is best represented as linear<sup>(7)</sup>. The linear rate may, in fact, be the result of some degree of exfoliation of these thickening scales, rather than a reflection of the intrinsic oxide growth rate. The scales formed consist of magnetite, and are initially double-layered with an essentially Cr-free outer layer and an inner layer in which Cr has accumulated to an extent dependent on the alloy Cr content. In laboratory experiments, Knödler and Ennis<sup>(8)</sup> found that

TABLE II  
LISTING OF PRIOR WORK  
(Supercritical conditions: 374.1°C, 217 atm, for pure water)

T°C	P, atm	Alloys	Author	Year	Ref.
286	1	C-steel	Vreeland, et al.	1962	13
286-500	1	C-steel	Pearl and Wozaldo	1965	14
400-550	1	C-steel	Potter and Mann	1963	6
482-621*	177-238	2.25Cr	Paterson, et al.	1992	7
499-541	104	2.25Cr	Griess, et al.	1978	15, 16
450-550	0.130-0.572	Fe, 2.25, 9Cr	Cory and Herrington	1987	9
450-550	1	Fe, 2.25, 9Cr	Mayer and Manolescu	1981	18
500	1	Type 304	Warzee, et al.	1965	19
500-550	0.18-0.2	2.25, 9Cr	Hurdus, et al.	1990	20
500-600	68-172	2.25, 9Cr	Banks, et al.	1984	21
500-900	1	Fe-15Ni-13 to 25Cr	Otsuka, et al.	1989	22
500-700	1	2.2-12Cr steels	Nava-Paz and Knodler	1998	23
538	238	ferritic steels; Ni-base	McCoy and McNabb	1977	24
550-700	1	9-12Cr steels	Fukuda, et al.	1995	25
550-750	1	2-12Cr steels	Fukuda, et al.	1998	26
560-700	10-99	2-11Cr steels	Watanabe, et al.	2000	27
600-650	100-200	Ni-Cr steels	Grishin, et al.	1969	28
600-650	1	Fe-9Cr	Itagaki, et al.	2000	29
600-800	1	Ni-Cr steels	Ericsson	1970	31, 32
649-816	1	Austenitic steels	Eberle and Anderson	1962	33
650	1	Ferritic steels	Knödler and Ennis	2001	8
650	0.5	Fe-9-12Cr, 316LN	Ennis, et al.	2001	34
650-700	1	Fe-11Cr	Murata, et al.	2001	35
700	1	Fe-base (16-18Cr); Ni-base	Otsuka and Fujikawa	1991	36
700	1	300-series, Ni-base	Ruther and Greenberg	1964	37
727-1127	0.1	Fe-9, 17Cr	Kusabiraki, et al.	1988	38
800	40	Inconel 600	Abe, et al.	1981	39
800	40	Ni-base	Abe and Yoshida	1985	40
700-1100	0.05-0.1	Fe-1 to 15Cr	Fujii and Meussner	1964	4
800-1200	0.1	Fe-0 to 10Cr	Wright and Wood	1969	5
900	0.2	Cr	Hultquist, et al.	2000	41

\*data calculated from in-plant measurements

alloy NF616/P92 exhibited parabolic oxidation up to 1500 h at 650°C (1202°F) in 1 atm steam, after which scale spallation led to a deviation from parabolic.

Parabolic Kinetics. Recent studies have tended to present the oxidation kinetics as parabolic. Parabolic rate constants calculated from plotting the literature data on mass gain-square root of time coordinates are presented in Figures 2a and 2b, for alloys with Cr contents in the range 0 to 2 percent, and 9 to 12 percent, respectively. It was assumed that the oxidation kinetics could be described by the usual relationship:

$$\text{Scale thickness} = A \cdot e^{-Q/RT} \cdot t^{1/n} \quad (1)$$

where  $Q$  is the activation energy for the rate-controlling process;  $T$  is the metal temperature (absolute);  $t$  is time,  $A$  is the Arrhenius constant; and  $R$  is the Gas Constant. For parabolic oxidation, the exponent  $n = 2$ , whereas for linear oxidation,  $n = 1$ . In the case of the dilute Cr alloys, there was good agreement among several sets of laboratory data and the field-derived data of Paterson, et al.<sup>(7)</sup> The trend of these data was best represented by a curve, or by two straight lines that intersected at approximately 500°C (932°F). The latter fit suggested a change in oxidation behavior with a significant increase in oxidation rate in the higher temperature regime.

The calculated activation energies for the two oxidation processes were 85 kJ/mole and 235 kJ/mole (below and above 500°C/932°F, respectively). The oxidation parameters from the best fits to these plots are summarized in Table III. For the dilute Cr alloys, Cory and Herrington<sup>(9)</sup> reported an activation energy of 163±15 kJ/mole for the formation of magnetite scales in steam over the narrow temperature range of 450-550°C (842-1022°F); the observed kinetics were parabolic after approximately 10h.

The good agreement between the two available data sets for the 9-12Cr alloys is shown in Figure 2b. These suggested that a single rate-controlling oxidation process operated over the whole temperature range studied, with an activation energy of 146 kJ/mole. This value is in good agreement with the 167±20kJ/mole (parabolic) reported for Fe-9Cr oxidized in steam at 475 and 550°C (887-1002°F) by Hurst and Cowen (report), and at 475-650°C (887-1202°F) by Eberle and Kitterman<sup>(10)</sup>, and McNary<sup>(11)</sup>; Manning<sup>(12)</sup> reported 153±18kJ/mole for the same temperature range.

Watanabe, et al.<sup>(27)</sup> reported much higher activation energies from high-pressure studies at 20 and 99 atm (290 and 1450 psi); for 2Cr steels the values were approximately 350 kJ/mole and 400 kJ/mole, respectively. For the 9-11Cr steels, the temperature dependence was essentially the same as that for the lower-Cr steels up to approximately 600°C (1112°F), but the oxidation rates at the higher temperatures were significantly lower than projected by that temperature dependence. At 700°C (1292°F) the oxidation rate decreased with increasing Cr content, the 11Cr alloy oxidizing noticeably slower than the 9Cr alloy. However, when compared with the data from other sources in Figure 2, Watanabe, et al.'s data points do not appear to be greatly separated from the line representing the best overall fit, so that the values of activation energy that they reported may have been unduly influenced by their relatively small data set.

Linear Kinetics. Further examination by the present authors of the data from some of the studies listed in Table II indicated that in many cases the oxidation behavior could be equally well represented by linear kinetics ( $R^2 > 0.95$ ); the rate constants so determined are presented for comparison in Figures 3a and 3b. For the 0-2Cr alloys, a single activation energy of 157 kJ/mole appeared to reasonably represent the data for temperatures above approximately 470°C (Figure 3a); at lower temperatures, the oxidation rate appeared to exhibit a lower temperature dependence. A fit of only the results from two laboratory studies that used Ar-0.1H<sub>2</sub>O gave a lower value of 113 kJ/mole. Note that in one of these studies<sup>(3)</sup> binary Fe-Cr alloys ranging from 1 to 15 percent Cr were considered to oxidize at essentially the same rate.

Figure 3b presents the linear kinetic data derived for Fe 9-12Cr alloys. If a single line were used to fit the data, an activation energy of 199 kJ/mole was obtained, whereas a fit of only the results from two laboratory studies that used Ar-0.1H<sub>2</sub>O gave the lower value of 103 kJ/mole.

Published values of the activation energy for the diffusion of Fe in FeO range from 105 to 155 kJ/mole<sup>(42)</sup>. Radiotracer measurements made during magnetite formation using <sup>55</sup>Fe at 500°C<sup>(43)</sup> yielded

an activation energy of  $163 \pm 15$  kJ/mole. Hauffe<sup>(44)</sup> reported an activation energy of 230 kJ/mole from diffusion measurements for Fe diffusion in  $\text{Fe}_3\text{O}_4$ , whereas oxidation of Fe to  $\text{Fe}_3\text{O}_4$  below  $570^\circ\text{C}$  yielded a value of 188 kJ/mole. Measurements of the self diffusion of Fe in  $\text{Fe}_2\text{O}_3$  gave an activation energy of 467 kJ/mole but, since this oxide is thought to grow by anion rather than cation transport, this latter activation energy probably is not relevant to oxidation behavior; oxidation of  $\text{Fe}_3\text{O}_4$  to  $\text{Fe}_2\text{O}_3$  was reported by Hauffe<sup>(44)</sup> to have an activation energy of 222 kJ/mole, presumably related to oxygen transport in the oxide.

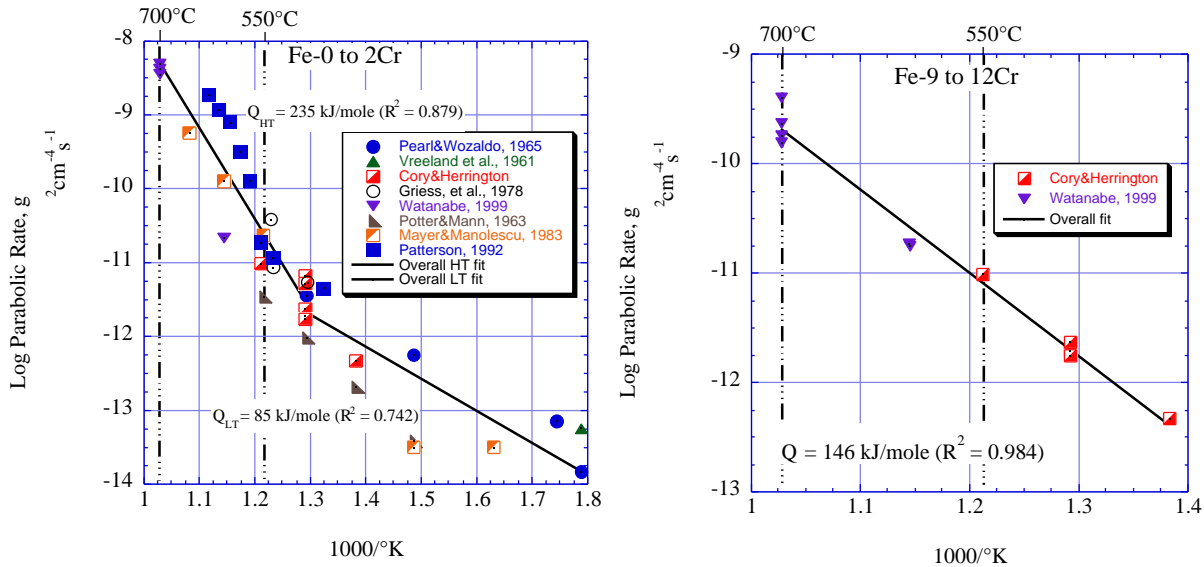


FIGURE 2. Arrhenius plots for the parabolic oxidation of (a) Fe-0 to 2Cr; and (b) Fe-9 to 12Cr

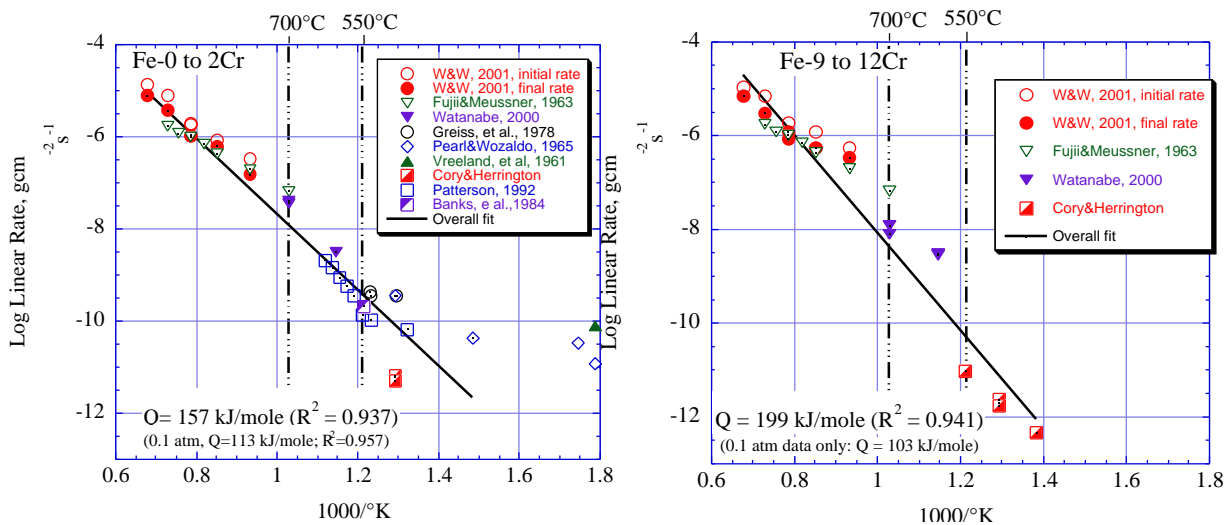


FIGURE 3. Arrhenius plots for the linear oxidation of (a) Fe-0 to 2Cr; and (b) Fe-9 to 12Cr

Overall, the activation energies determined from the assumption of parabolic kinetics for both alloy sets do not provide any clear-cut indication of the rate-controlling mechanism, since they fall into the top of the range reported for Fe diffusion in  $\text{FeO}$ , and into the bottom of the range for Fe diffusion in  $\text{Fe}_3\text{O}_4$ . When linear kinetics are assumed, the results for the 0-2Cr alloys straddle the values for Fe

diffusion in FeO. The activation energy from overall fit of linear kinetics for the 9-12Cr alloys was typical of those reported for Fe diffusion in Fe<sub>3</sub>O<sub>4</sub>, whereas the activation energies from consideration of only the Ar-0.1 water vapor data were lower than this.

The oxidation parameters derived from these Arrhenius plots were used to make comparisons of the relative amounts of oxide growth expected, assuming parabolic or linear oxidation behavior. The mass gains and corresponding oxide thicknesses (assuming no scale spallation) expected in the nominal plant lifetime of 250kh are summarized in Table III, using as an example an average metal temperature of 650°C (1202°F) and no effect of steam pressure. Spallation would result in regrowth of oxide at a rate that, in the case of parabolic kinetics, would depend on the thickness of the remaining oxide so that the ensuing rate would be faster than that before spallation. Nevertheless, the assumption of linear oxidation kinetics clearly results, as expected, in a very significant increase in oxide growth that would result in much shorter lifetimes than would be obtained from an assumption of parabolic kinetics.

TABLE III  
SUMMARY OF OXIDATION RATES

Alloy	Temperature Range °C	Oxidation Parameters <sup>a</sup>		After 250kh at 650°C	
		A	Q, kJ/mole	mass gain (mg/cm <sup>2</sup> )	oxide thickness <sup>b</sup> (µm)
		Parabolic Oxidation <sup>c</sup>			
0 to 2Cr	500-700	2.10 x 10 <sup>4</sup>	235	977	520
9 to 12Cr	450-700	1.42 x 10 <sup>-2</sup>	146	263	140
		Linear Oxidation <sup>d</sup>			
0 to 2Cr	470-1200	3.70	157	4,332	2,307
	700-1200 <sup>b</sup>	5.5 x 10 <sup>-2</sup>	113	19,914	10,605
9 to 12Cr	450-1200	230.5	199	1,133	603
	700-1200 <sup>b</sup>	1.28 x 10 <sup>-2</sup>	103	17,059	9,085

<sup>a</sup> from  $k = A \cdot e^{-Q/RT}$

<sup>b</sup> assuming oxide is all magnetite (  $\rho = 5.18 \text{ gcm}^{-3}$  )

<sup>c</sup> A in  $\text{g}^2\text{cm}^{-4}\text{s}^{-1}$

<sup>d</sup> A in  $\text{gcm}^{-2}\text{s}^{-1}$

<sup>e</sup> lab. data for Ar-0.1H<sub>2</sub>O only

#### Effect of Steam Pressure

The fact that the bulk of experimental work on steam oxidation has been made at steam pressures significantly lower than those contemplated in advanced power plants, with a number of studies employing steam pressures less than 1 atm, raises a question about the applicability of the results to full supercritical steam conditions. Watanabe et al.<sup>(27)</sup> reported only a small effect of pressure over the range 10 to 99 atm on the oxidation rates of 2 and 9-11Cr alloys at 700°C (1292°F), while at 600°C (1112°F) and below the value of the oxidation rate constant decreased with increasing pressure. However, the activation energies reported from this work are much higher than those reported by others, suggesting that the rate-controlling mechanisms might be different than at the lower pressures. From low-pressure studies in Ar-water vapor mixtures, Fujii and Meussner<sup>(3)</sup> reported a strong pressure dependence in the temperature range 800 to 1100°C (1472 to 2012°F), with the oxidation rates increasing when the P<sub>H<sub>2</sub>O</sub> was increased from 0.05 to 0.10 atm.

The relationships used in procedures for back-calculating average tube temperature from oxide thickness measurements<sup>(7)</sup> generally use an exponent of 0.20 to 0.38 for the dependence on total steam pressure ( $P$ ):

$$\text{i.e., oxide thickness} = f(A \cdot P^{(0.20-0.38)} \cdot e^{-Q/RT}) \quad (2)$$

This suggests that, at any given temperature and assuming the other factors are unaffected by pressure, increasing the total steam pressure from 177 to 238 atm would increase the scale thickness by a factor of 1.06 to 1.12, whereas increasing the steam pressure from 177 to 340 atm would increase the oxide thickness by factors of 1.14 to 1.28.

A further way in which steam pressure could affect oxidation behavior is through the dissolution of impurities in the steam. Unintended impurities resulting from, for example, condenser in-leakage could allow impurities to enter the feedwater and possibly be taken up in the steam. Supercritical steam has an appreciable solubility for impurities, such as silica for instance. Any effect of such impurities in steam on the oxidation behavior of the steam-touched alloys is not known.

In terms of reconciling laboratory studies in environments such as Ar-0.1 H<sub>2</sub>O, if this relationship is applicable to lower pressures, equation 2 suggests that the laboratory-oxidation kinetics will underestimate the oxidation rate by factors of 3 to 9 (1 atm) or 5 to 22 (0.1 atm). Given the apparently reasonable correspondence of the laboratory data with the higher-pressure data shown in Figs. 2 and 3, the applicability of this relationship to lower pressures appears doubtful.

## OXIDE SCALE MORPHOLOGIES

Double-layered magnetite scales have been reported to form on the lower-Cr ferritic steels in studies of tubing removed from operating boilers<sup>(7)</sup>, as well as in laboratory studies. Surman and Castle<sup>(45)</sup> observed the formation of both single-layered and duplex scales on 99.99 percent Fe in water vapor, and that the rate of scale growth was parabolic when a duplex scale was formed, but faster when a single layer was formed. Mayer and Manolescu<sup>(18)</sup> described the formation of double-layered scales on dilute Fe-Cr alloys in steam, with an outer layer of magnetite characterized by a columnar grain structure with pores at grain boundary triple points, and an inner layer of magnetite with an equiaxed grain structure with irregular porosity, apparently in rows parallel to surface, as well as Fe-Cr spinel at its innermost surface. The ratio of the thicknesses of the inner and outer layers was independent of time, but increased with increasing alloy Cr content.

Cory and Herrington<sup>(9)</sup> reported that both layers of the two-layered scales formed on Fe-2.25Cr and Fe-9Cr alloys were magnetite, and that the interface between the layers corresponded to the original metal surface. The scales had a laminated appearance, which had also been seen by Hurst and Cowen<sup>(46)</sup>, with alternating bands of dense and porous scale suggestive of formation by plastic deformation and collapse. The scales were less porous than reported earlier<sup>(18)</sup>, but the outer layer was more porous than the inner. On the Fe-9Cr alloy, internal oxidation along surface grain boundaries occurred; the depth of penetration was temperature-dependent, so that the observed good Arrhenius behavior of this alloy (see Figure 2b) may have been fortuitous. These authors also suggested that Si in the alloy made a larger contribution to the protective nature of the scale than did Cr, but such a trend is difficult to judge.

Watanabe, et al.<sup>(27)</sup> found that under all testing conditions [560°C and 700°C (1040 and 1292°F);

10 and 99 atm (145 and 1450 psi) total pressure], duplex scales were formed on alloys containing 2 and 9-11Cr. As found in other studies, both layers were basically magnetite; the outer layer was Cr-free whereas the inner layer was enriched in Cr, which became more pronounced for the 9-11 Cr steels at the higher testing temperatures. The inner layer of the 11Cr alloy exposed to 700°C/99 atm steam contained over 40 percent Cr, which was considered to provide an effective diffusion barrier. While the maximum Cr contents of the inner layers on the 9-11Cr steels increased with temperature, especially above 600°C (1112°F), the maximum Cr concentration for the 2Cr steel remained below 13 percent. In both the higher-Cr alloys, a layer of internal oxide particles was observed beneath the inner oxide layer; such layers were more apparent at the lower temperatures. There was no clear effect of Cr concentration on the parabolic rate constant at 570 and 620°C (1058 and 1148°F), but at 700°C there appeared to be an almost linear decrease, in keeping with the increasing maximum Cr content inner layer.

Itagaki et al.,<sup>(29)</sup> reported the formation of a thin Cr-rich oxide, with no evidence of magnetite formation, on a 9Cr-based alloy (NF616) to which an addition of 3 percent Pd had been made, and significantly improved oxidation resistance in steam at 650°C (1202°F). These authors also found that additions of up to 1 percent Si to the base alloy improved oxidation resistance, but that the Si additions accelerated carbide agglomeration in the fully martensitic structure, so degrading long-term creep rupture strength. Preoxidation of this Si-modified alloy in an Ar-O<sub>2</sub> mixture also greatly improved its oxidation resistance in steam at 700°C in 1000 h tests.

Studies of the oxidation behavior of 99.997 percent Cr in 0.2 atm water vapor, oxygen, and air provided some insight to the potential effects of steam on the oxidation behavior of alloys capable of forming chromia scales<sup>(41)</sup>. The oxidation rate in water vapor was twice as fast as in O<sub>2</sub>, due to effects of H on the transport properties of the oxide, and to the formation of the volatile chromium oxy-hydroxide, CrO<sub>2</sub>(OH)<sub>2</sub>. Oxide growth occurred in both the outer and inner parts of the oxide. In water vapor, the fraction of growth at the inner surface (29-38 percent) led to a flat metal-oxide interface and good oxide adherence; in O<sub>2</sub>, the fraction of growth at the inner surface was 18 percent for Cr that had been charged with hydrogen, and bucking of the interface occurred with poor oxide adherence.

#### Scales Grown in Ar-0.1 Water Vapor

Oxidation of Fe-Cr alloys in Ar-0.1 water vapor produced scales that were essentially two-layered, but the oxide was wustite (FeO, not magnetite)<sup>(3,5,38)</sup>. The gas side of the outer layer was massively faceted on all the alloys studied (0-15Cr), so that its thickness was very non-uniform. The inner oxide layer was relatively uniform in thickness on alloys containing more than 1 percent Cr, and thickened at a linear rate which increased with increasing alloy Cr level, even though the overall oxidation rates of the alloys were essentially the same. The inner layer consisted of internal (Cr<sub>2</sub>O<sub>3</sub>) particles that appeared to be incorporated by the inward-growing scale with the same spatial distribution that they had in the alloy. With increasing time and temperature, the incorporated internal oxide particles dissolved in the inner FeO layer and the Cr level of the inner layer increased with increasing alloy Cr level. The Cr level of the outer FeO layer was very low, and did not increase much with increasing time, temperature, or alloy Cr level. Despite the similar oxidation rates and morphologies of the scales formed on all the alloys, the relative thickness of the inner (Cr-containing) scale to the outer FeO layer increased with increasing Cr content. With continued oxidation, at some oxide thickness the outer FeO separated from the alloy (on Fe) or from the inner scale (on all the alloys) and multiple FeO layers formed. The outer surfaces of each of these separated layers were also faceted, but did not match the inner surface facets of the next outer layer. The inner surface of the innermost separated FeO was observed to have growth (or dissociation) steps/ledges.

## OXIDATION MECHANISMS

Oxidation studies using steam containing  $^{18}\text{O}$  have shown that magnetite layers in steam grow simultaneously at both the oxide-gas and the metal-oxide interfaces<sup>(31,32)</sup>. A common finding in many of the studies of oxidation in steam or water vapor is that the scales exhibit significant porosity, to the extent that the suggested oxidation mechanisms invoke transport of Fe out and steam in via an interconnected pore network. Surman and Castle<sup>(45)</sup> suggested that Fe was transported in the vapor phase (via the volatile species  $\text{Fe}(\text{OH})_2$ ) through pores and cavities from the metal-oxide interface to the outer layer. However, Cory and Herrington<sup>(9)</sup> pointed out that Co and Ni hydroxides have similar volatilities, and remained in the inner layer. Mayer and Manolescu<sup>(18)</sup> agreed with Surman and Castle<sup>(45)</sup> on the importance of vapor-phase transport, and considered that two possible mechanisms may operate: vapor-phase transport, or provision for the growth of the inner layer by dissociation of the outer layer.

At temperatures only slightly higher than those currently envisioned in steam power plants, two laboratory studies in Ar-0.1 water vapor<sup>(3-5)</sup> suggested that the oxidation behavior was not controlled by diffusion through the scales. The strong pressure dependence of oxidation in Ar-water vapor mixtures, the low activation energy, and the peculiar scale morphologies were taken to indicate that the rate-controlling process occurred at the gas-oxide interface. However, the observations that one side of the scale on pure Fe was forced to lift by the retreating core, and that the lifted side did not continue to thicken at the same rate as the adherent side suggests that, in the absence of the oxygen demand from Cr, the rate of O transport inwards is very slow. In contrast, a study under similar conditions<sup>(38)</sup> in which FeO layers with essentially the same oxide morphologies were formed represented the oxidation kinetics as parabolic. The observation from the review of the overall available data that the oxidation rates at the higher temperatures are fast, and not very different for the 2Cr and 10-12Cr alloys (see Figs. 2 and 3, and the estimated oxide growth at 650°C in Table III), is very similar to those made in the Ar-0.1 water vapor laboratory studies.

Watanabe, et al.<sup>(27)</sup> measured similar activation energies for pure iron and Fe-2Cr, suggesting that this level of Cr does not have a significant effect on the rate-determining process. These authors attributed the slower oxidation rate of HCM12A compared to NF616 to the 2 percent increase in Cr level; the Si contents of these two steels were noted to be very similar. Itagaki et al.<sup>(29)</sup> found useful improvement in the oxidation resistance of a 9Cr alloy by additions of Si, but these additions led to the development of detrimental interactions with the alloy strengthening mechanisms at long times. The same authors also reported a 1.3x increase in mass gain when W was substituted for Mo in 9Cr-based alloys, whereas Watanabe, et al.<sup>(26)</sup> reported that an addition of 1.6 percent W to the 2Cr steel made no difference to the oxidation rates in their tests.

## DISCUSSION

It is apparent that the available data for oxidation of dilute Fe-Cr alloys in steam can be described relatively well by both parabolic and linear kinetics. If, in fact, parabolic kinetics prevail, any tendency of the scale to spall at increased thicknesses/longer times would render questionable the use of a parabolic scale growth rate law in any life prediction calculations. In that case, practical life prediction efforts probably would opt for the use of an effective linear overall rate of scale growth (probably determined empirically from gross overall measurements), to provide an acceptable degree of conservatism.

An alternative approach that could improve alloy utilization would be to develop the ability to accurately describe the actual oxidation behavior, and to use this for life prediction. This approach

would involve understanding and modeling the various stages of the oxidation process, which may include: oxide growth according to parabolic or linear kinetics to some critical thickness at which spallation becomes possible, followed by periodic loss of scale involving loss of specific layers, over specific parts of the component surface. Such modeling is in progress for relatively simple alloys oxidized in air<sup>(47,48)</sup>, and the efforts so far show excellent promise.

For the higher-Cr alloys a major question is the ability to form a scale that will provide acceptable protection at the higher temperatures. While there appears to be some disagreement about the influence of Si on oxidation behavior in steam, the effectiveness of small additions of Si is worthy of further examination in view of recent findings of the development of an apparently rate-controlling sublayer of SiO<sub>2</sub> on a fine-grained Fe-13Cr, low-Si alloy<sup>(49)</sup>. Other small changes, such as preoxidation<sup>(38)</sup>, or the addition of 50 ppm S<sup>(35)</sup> also have been shown to improve the oxidation behavior.

## CONCLUSIONS AND REMAINING QUESTIONS

The low-Cr alloys exhibit relatively high rates of oxidation in steam, as is expected since they form magnetite-rich scales. While similar scales and oxidation rates are observed for the higher-Cr alloys, there appears to be the possibility of forming relatively protective scales on the 12Cr alloys. The effects of changes in the alloy compositions to increase long-term creep strength must be better understood, as well as the effects of the oxidation process on alloy microstructure and mechanical properties. There is some indication that modifications that can promote the formation of a basal oxide layer that can act as a diffusion barrier to the species involved in the oxidation process, or can promote increased transport of Cr to the alloy surface, may result in a significant reduction in the oxidation rate of the 9-12Cr alloys. Routes by which rapid transport of Cr to the alloy surface can be facilitated, such as by surface cold work<sup>(50)</sup> or by a very small alloy grain size<sup>(49)</sup>, have been shown to promote Cr-enriched scale formation, at least during initial exposure. While such effects were not particularly featured in the research reviewed, their applicability should be considered in future studies. There also remains the possibility of doping the inner magnetite layer formed on the lower-Cr alloys in steam to reduce the rate of Fe diffusion. However, this would only be effective if the rate-controlling step in the oxidation process involved cation diffusion; it is not clear from the available data if and under what conditions this is the case.

The changes in steam pressure from the current levels to those planned in future steam generators appear likely to have only a small effect on the oxidation rate of these alloys. The implications for laboratory studies are that there should not be a need to conduct oxidation experiments at elevated pressures unless the oxidation behavior is limited by the rate of arrival of the oxidizing species at the oxide-gas interface (steam flow rate), and/or by the rate at which the water vapor can dissociate. There is a strong indication that the slowest step in the oxidation rate at temperatures of 700°C and higher in Ar-0.1 water vapor atmospheres is, in fact, the availability of oxygen, so that it would appear that laboratory testing would be best done in steam at 1 atm unless it can be shown that similar oxide scale morphologies are formed in high-pressure steam and 0.1 atm water vapor. There is a need for more complete correlation between oxidation kinetics and the detailed morphology of the scales formed to provide improved understanding of the mode of oxidation and any changes with temperature.

Overall, the apparent ambiguity of some of the available laboratory data suggests that reliable extrapolation of relatively short-term laboratory data to estimate the rate of steam-side degradation of ferritic steel tubes in operating power plants is not possible at present. The practical observation of a change in oxidation kinetics with time, together with the effects of thermal cycling, heat transfer across the oxide layers, and possible effects of impurities in the steam are factors that must be understood

before such estimations can be made. In addition, the effect of higher tube wall temperatures on corrosion on the fireside of the tubes also must be considered, and may prove to limit service life more than steam-side oxidation.

## ACKNOWLEDGEMENTS

This work was carried out as part of program FEAA061, "Materials for Ultra-Supercritical Steam Power Plants," funded by the U.S. Department of Energy under contract no. DE-AC05-00OR22725 with UT-Battelle LLC. The authors are grateful to colleagues at the Oak Ridge National Laboratory, especially Drs. J. C. Griess and R. W. Swindeman, for input and helpful discussions. This program is part of an overall DOE- and Energy Industries of Ohio-funded program on "Boiler Materials for Ultrasupercritical Coal Power Plants," and the authors are also grateful to members of the consortium participating in this program for review and comment on the paper.

## REFERENCES

1. M. Staubli, K. H. Mayer, T. U. Kern, R. W. Vanstone, R. Hanus, J. Stief, and K. H. Schönfeld, paper 1.3, presented at the 3<sup>rd</sup> EPRI Conference on Advances in Materials Technologies for Fossil Power Plants, Swansea, 2001.
2. F. Abe, M. Igarashi, S. Wanikawa, M. Tabuchi, T. Itagaki, K. Kimura, and K. Yamaguchi, pp. 129-Century Turbines and Power Plant, A. Strang, W. M. Banks, R. D. Conroy, G. M. McColvin, J. C. Neal, and S. Simpson, Eds., IOM Communications Ltd., London, Book 736 (2000).
3. C. T. Fujii and R. A. Meussner, *J. Electrochemical Soc.*, 110 (12), 1195-1204 (1963).
4. C. T. Fujii and R. A. Meussner, *J. Electrochemical Soc.*, 111 (11), 1215-1221 (1964).
5. I. G. Wright and G. C. Wood, unpublished work on dilute Fe-Cr alloys, 1969.
6. E. C. Potter and G. M. W. Mann, pp. 872-879 in Proc. 2<sup>nd</sup> Intl. Congress on Metallic Corrosion (1963).
7. S. R. Paterson, R. Moser, and T. R. Rettig, pp. 8-1-8.5 in Proc. Int. Conf. on Interaction of Iron-Based Materials with Water and Steam, R. B. Dooley and A. Bursik, Eds., EPRI Report No. TR-102101 (1992).
8. R. Knödler and P. J. Ennis, Proc. Baltica V Conference 2001: Condition Assessment of Power Plant, Porvoo, Finland, 6-8 June 2001, pp 355-364 in Vol. 1.
9. N. J. Cory and T. M. Herrington, *Oxidation of Metals*, 28 (5/6), 237-258 (1987).
10. F. Eberle and J. M. Kitterman, in Behavior of Superheater Alloys in High-Temperature, High-Pressure Steam, G. E. Lien, Ed., ASME, New York (1968).
11. T. A. McNary, Babcock & Wilcox Research Report No. 7724, Alliance, Ohio (1966).
12. M. I. Manning, CERL Report No. RD/L/N 125 (1977).
13. D. C. Vreeland, G. G. Gaul, and W. L. Pearl, *Corrosion*, 18, 368t-377t (1962).
14. W. L. Pearl and G. P. Wozaldo, *Corrosion*, 21, 260-267 (1965).
15. J. C. Griess, J. M. Devan, and W. A. Maxwell, *Materials Performance*, 17, 9 (1978).
16. J. C. Griess, J. M. Devan, and W. A. Maxwell, *Materials Performance*, 18-24 (1982).
17. J. M. Perrow and W. W. Smeltzer, *J. Electrochemical Soc.*, 109, 1023 (1962).
18. P. Mayer and A. V. Manolescu, pp. 368-379 in High-Temperature Corrosion, Ed. R. A. Rapp, NACE, Houston, Texas (1983).
19. M. Warzee, J. Hennaut, M. Maurice, C. Sonnen, J. Waty, and P. Berge, *J. Electrochemical Soc.*, 112, 670 (1965).
20. M. H. Hurdus, L. Tomlinson, and J. M. Titchmarsh, *Oxidation of Metals*, 34 (5/6), 429-464 (1990).
21. P. Banks, J. H. B. Lowick, and P. Hurst, UKAEA Report No. ND-R-1012R, 1984.
22. N. Otsuka, Y. Shida, and H. Fujikawa, *Oxidation of Metals*, 32 (1/2), 13-45 (1989).

23. J. C. Nava-Paz and R. Knodler, pp. 451-459 in Materials for Advanced Power Engineering 1998, J. Lecomte-Beckers, F. Schubert, and P. J. Ennis, Eds., Forschungszentrum Jülich GmbH (1998).
24. H. E. McCoy and B. McNabb, Report ORNL/TM-5781, 1977
25. Y. Fukuda, K. Tamura, and K. Suzuki, Int. Symp. on Plant Aging and Life Prediction of Corrodible Structures, Sapporo, Japan, 1995.
26. Y. Fukuda, K. Tamura, and T. Sato, pp. 461-469 in Materials for Advanced Power Engineering 1998, J. Lecomte-Beckers, F. Schubert, and P. J. Ennis, Eds., Forschungszentrum Jülich GmbH (1998).
27. Y. Watanabe, Y.S. Yi, T. Kondo, K. Inui, T. Kishinami, and H. Kimura, M. Sato, pp. 545-552 in Proceedings of the Ninth International Conference on Pressure Vessel Technology, ICPVT-9, Sydney, Australia, 9-14, April 2000, ISBN0-7337-3353-0.
28. A. M. Grishin, V. G. Perkov, V. P. Sentyurev, and Y. Y. Yashchenko, *Thermal Engineering*, 16, 121 (1969).
29. T. Itagaki, H. Kutsumi, M. Igarashi, and F. Abe, *ISJI*, 13, 1114-1115 (2000); quoted in Abe, et al., 2001.
30. F. Abe, M. Igarashi, S. Wanikawa, M. Tabuchi, T. Itagaki, K. Kimura, and K. Yamaguchi, paper 2.2, presented at the 3<sup>rd</sup> EPRI Conference on Advances in Materials Technologies for Fossil Power Plants, Swansea, 2001.
31. T. Ericsson, *Oxidation of Metals*, 2, 173 (1970).
32. T. Ericsson, *Oxidation of Metals*, 2, 401 (1970).
33. F. Eberle and C. H. Anderson, *Trans. ASME, J. Engineering for Power*, 223 (1962).
34. P. J. Ennis, Y. Wouters, and W. J. Quadackers, pp. 457-467 in Advanced Heat-resistant Steel for Power Generation, R. Viswanathan and J. Nutting, Eds., IOM Communications Ltd., London, Book 708 (2001).
35. Y. Murata, M. Morinaga, R. Hashizume, Y. Sawaragi, and M. Nakai, paper 9.1, presented at the 3<sup>rd</sup> EPRI Conference on Advances in Materials Technologies for Fossil Power Plants, Swansea, 2001.
36. N. Otsuka and H. Fujikawa, *Corrosion*, 47 (4), 240-248 (1991).
37. W. E. Ruther and S. Greenberg, *J. Electrochemical Soc.*, 111, 1116-1121 (1964).
38. K. Kusabiraki, H. Toki, and K. Asami, *Tetsu-to-Hagane*, 74, 863-878 (1988).
39. F. Abe, H. Araki, H. Yoshida, M. Okada, and R. Watanabe, *Corrosion Science*, 21 819 (1981).
40. F. Abe and H. Yoshida, *Z. Metallkunde*, 76 (3), 219-225 (1985).
41. G. Hultquist, B. Tveten, and E. Hörnlund, *Oxidation of Metals*, 54 (1/2), 1-10 (2000).
42. C. E. Birchenall, pp. 119-127 in Mass Transport in Oxides, National Bureau of Standards Special Publication 296, Washington (1968).
43. A. Atkinson and R. I. Taylor, *J. Materials Science*, 18, 2371 (1983).
44. K. Hauffe, pp. 280-282 in Oxidation of Metals, Plenum Press, New York (1965).
45. P. L. Surman and J. E. Castle, *Corrosion Science*, 9, 771 (1969).
46. P. Hurst and H. C. Cowan, paper no. 62 in Proc. International Conference on Ferritic Steels for Fast Breeder Steam Generators, British Nuclear Energy Soc., London (1977).
47. J. R. Nicholls and M. J. Bennett, Paper No. 1 in Proc. European Federation of Corrosion Workshop on Lifetime Modeling of High-Temperature Corrosion Processes, EFC Series Vol. 27 (2001).
48. I. G. Wright, B. A. Pint, L. M. Hall, and P. F. Tortorelli, paper No. 25 in Proc. European Federation of Corrosion Workshop on Lifetime Modeling of High-Temperature Corrosion Processes, EFC Series Vol. 27 (2001).
49. D. T. Hoelzer, B. A. Pint, and I. G. Wright, *J. Nuclear Materials*, 283-287, 1306-1310 (2000).
50. A. Rahmel, *Z. Elektrochem.*, 66, 363 (1962).